Generalized derivation of the added-mass and circulatory forces for viscous flows

Eric Limacher,* Chris Morton, and David Wood
Department of Mechanical and Manufacturing Engineering, University of Calgary, 2500 University Drive NW, Calgary, Alberta, Canada T2N 1N4

(Received 12 July 2017; published 17 January 2018)

The concept of added mass arises from potential flow analysis and is associated with the acceleration of a body in an inviscid irrotational fluid. When shed vorticity is modeled as vortex singularities embedded in this irrotational flow, the associated force can be superimposed onto the added-mass force due to the linearity of the governing Laplace equation. This decomposition of force into added-mass and circulatory components remains common in modern aerodynamic models, but its applicability to viscous separated flows remains unclear. The present work addresses this knowledge gap by presenting a generalized derivation of the added-mass and circulatory force decomposition which is valid for a body of arbitrary shape in an unbounded, incompressible fluid domain, in both two and three dimensions, undergoing arbitrary motions amid continuous distributions of vorticity. From the general expression, the classical added-mass force is rederived for well-known canonical cases and is seen to be additive to the circulatory force for any flow. The formulation is shown to be equivalent to existing theoretical work under the specific conditions and assumptions of previous studies. It is also validated using a numerical simulation of a pitching plate in a steady freestream flow, conducted by Wang and Eldredge [Theor. Comput. Fluid Dyn. **27**, 577 (2013)]. In response to persistent confusion in the literature, a discussion of the most appropriate physical interpretation of added mass is included, informed by inspection of the derived equations. The added-mass force is seen to account for the dynamic effect of near-body vorticity and is not (as is commonly claimed) associated with the acceleration of near-body fluid which "must" somehow move with the body. Various other consequences of the derivation are discussed, including a concept which has been labeled the conservation of image-vorticity impulse.

DOI: 10.1103/PhysRevFluids.3.014701

I. INTRODUCTION

One of the most familiar decompositions of aerodynamic force splits the total force into added-mass and circulatory components. Perhaps the most famous examples are the classical works of Theodorsen [1] and von Kármán and Sears [2], wherein the vorticity field is represented by vortex sheets. When the shed vorticity is confined to singularities embedded in an otherwise irrotational flow, the added-mass force can be superimposed onto the force associated with the shed vorticity due to the linearity of the governing Laplace equation. The key aim of the present study is to demonstrate how this decomposition can be generalized to viscous flows containing continuous distributions of vorticity. As a background to this problem, the history of the concepts of added-mass and circulatory force are briefly recounted in this introductory section.

*ejlimach@ucalgary.ca

The concept of added mass can be traced back to the nineteenth century. In 1851, Stokes [3] reviewed the literature on how a fluid imparts extra inertia—not yet termed "added mass"—to a submerged oscillating pendulum, thereby increasing its period relative to the value expected in a vacuum. The force on a body in a vacuum will be proportional to the body's mass M and its instantaneous acceleration $\dot{\mathbf{U}}$ as per Newton's second law. A submerged body will experience an additional force proportional to the rate at which the body imparts momentum to the surrounding fluid. Under the assumptions of an irrotational flow around a linearly accelerating body without rotation, this additional force can be shown to be proportional to the instantaneous acceleration of the body (see, e.g., [4]). Taking the constant of proportionality to be m', the total force $\mathbf{F}_{\text{tot}}$ can be expressed as

$$\mathbf{F}_{\text{tot}} = -(M + m')\dot{\mathbf{U}}, \tag{1}$$

from which m' is easily interpreted as an additional mass that must be accelerated with the body. In different works, m' can be referred to as added mass [4], apparent mass [5], or virtual mass [6].

An expression for m' is derived using potential flow analysis, whereby the velocity field is expressed as $\mathbf{u} = \nabla\phi$ and ϕ is a single-valued scalar potential. For incompressible flows, ϕ is the solution to the Laplace equation $\nabla^2\phi = 0$, subject to the impermeable boundary condition at the body surface. In a frame of reference where velocity decays to zero at infinity, conservation of energy can be used to show that [4]

$$m' = \rho \int_V \frac{u^2}{U^2} dV, \tag{2}$$

where u is the velocity at any point within the fluid volume V and U is the instantaneous body velocity. For one-dimensional linear translation, m' is constant, as the velocity u scales proportionally everywhere with U. In three dimensions, taking $\dot{\mathbf{U}}$ to represent the instantaneous acceleration of the body centroid, the added-mass force can be expressed as [7]

$$\mathbf{F}_{am} = -\mathbf{M}_{ij}\dot{\mathbf{U}}, \tag{3}$$

where $\mathbf{M}_{ij}$ is a 3×3 diagonal matrix. The elements of $\mathbf{M}_{ij}$ are not generally equal and depend on the orientation of the coordinate system relative to the body. Once body rotation is considered, force components arise which depend on the product of rotation rate and translational velocity; it is here that the analogy to additional inertia breaks down.

The force associated with the scalar potential is [6]

$$\mathbf{F}_{am} = -\rho \frac{d}{dt} \oint_{S_b} \phi \hat{n}\, dS, \tag{4}$$

where $\hat{n}$ is an outward-facing unit normal on the body surface S_b. Saffman [6] refers to the integral in Eq. (4) as the virtual momentum of the body and notes that previous authors such as Lamb [8] called it the impulse of the fluid. This integral will arise in the derivation in the following section, with special care taken as to the frame of reference in which ϕ is defined. The generic term *impulse* has taken on a different meaning in modern aerodynamic literature, often referring specifically to the momentum associated with the vortical component of the flow field (see, e.g., [6]).

A common physical interpretation of the added-mass force attributes it to the acceleration of fluid around the body (see, e.g., [9,10]). Of course, the total force on the body, not only the added-mass force, is due to the acceleration of the surrounding fluid by the principle of momentum conservation. Colloquially, it is sometimes said that the added-mass force accounts for the acceleration of fluid *near* the body, which *must* move with it. There is, in fact, no identifiable finite volume of fluid within the assumed irrotational flow field which accelerates with the body to give rise to this force [4]; all fluid around the body, extending outward to infinity, is accelerated to some degree. Aside from its physical inaccuracy, this common interpretation does not help to understand when the added-mass force should be included in an expression of total force and it is limited in its ability to predict when

the added-mass force will be the dominant component of total force. These practical concerns will be considered in the present work.

Having inherited a well-developed theory of added-mass force, it would be convenient to express the total force for more general cases as the sum of the added-mass force and some residual force. Since rotational effects are neglected in the derivation of added mass, it stands to reason that the residual force can be attributed to the vorticity field. The notion of momentum associated with vortices can be traced back to the 1883 treatise by Thomson [11] in which he presents an expression for the vortex momentum of a ring vortex. von Kármán and Sears [2] describe a force arising from the separation of point vortex pairs from one another, stating this idea as a well-known fact without citation. Wu *et al*. [12] tell us that Burgers [13], Wu [5], and Lighthill [14] all independently derived a general expression for the force arising from the vorticity field, relating it to the first moment of vorticity,

$$\int_V \mathbf{x} \times \boldsymbol{\omega}\, dV, \tag{5}$$

where $\mathbf{x}$ is a position vector, $\boldsymbol{\omega}$ is the vorticity, and V is the volume occupied by fluid. In Lighthill's derivation, this expression is related to the total impulse necessary to establish a vortical flow field from rest. The term *impulse* has since been co-opted to refer specifically to this integral, which can also be referred to as hydrodynamic impulse [6] or vortical impulse [12]. The time derivative of impulse, defined in this way, gives rise to a force.

Nonetheless, it is not immediately apparent how to combine this component of force with the previously discussed added-mass force. The force formula of Wu [5] includes the time derivative of impulse, but does not include an added-mass force. Rather, the total force on a solid body submersed in an unbounded incompressible fluid domain is given as

$$\mathbf{F} = -\rho \frac{1}{N-1} \frac{d}{dt} \int_V \mathbf{x} \times \boldsymbol{\omega}\, dV + \rho \frac{d}{dt} \int_{V_b} \mathbf{u}\, dV, \tag{6}$$

where $N = \{2,3\}$ is the dimension of the space and $\mathbf{u}$ is the velocity of the body at any point within the body volume V_b. Lin and Rockwell [15] applied the concept of impulse to calculate force from a vorticity field determined experimentally using particle image velocimetry (PIV). For an oscillating cylinder, they calculated the total force from the time derivative of impulse, citing Lighthill [14], but omitting the second term in Eq. (6).

Lighthill [7] proposed an added-mass and circulatory force decomposition in an attempt to generalize the Morison equation. The Morison equation expresses the force on marine structures as the sum of the quasisteady drag component (proportional to the instantaneous square of incident velocity) and another component proportional to the instantaneous acceleration of the body or freestream [4]. The latter term is derived from potential flow analysis and the former arises from continuous vortex shedding. Lighthill [7] postulated that the drag term arising from the steady flow, typically expressed in terms of a steady drag coefficient, could be replaced by an expression involving the impulse in Eq. (5). The force acting on an accelerating body in a steady freestream flow in three dimensions would thus be given as

$$\mathbf{F} = -\frac{1}{2}\rho \frac{d}{dt} \int_V \mathbf{x} \times \boldsymbol{\omega}\, dV - \mathbf{M}_{ij}\dot{\mathbf{U}}. \tag{7}$$

In Lighthill's treatment, the vorticity in the impulse integral must include only what he terms the additional vorticity, defined as the complete vorticity distribution in the volume V minus the vortex sheet associated with the tangential slip velocity along S_b for an acyclic potential flow around the body. In Sec. VIII C, this peculiar concept will be discussed and the force decomposition to be derived herein will be shown to be equivalent to Eq. (7).

With the advent of optical experimental techniques such as PIV, several other force decompositions have been derived to express the total force on a body in terms of the velocity and vorticity fields for use with such data sets (see, e.g., [16–18]; for a more thorough review of various decompositions,

see [19]). However, none of the force decompositions in these works include an added-mass force. By contrast, many, if not most, contemporary aerodynamic models still include added-mass as a force component (see, e.g., [20–23]). These works are essentially extensions of the theoretical approach of Theodorsen [1] and von Kármán and Sears [2]. The experimental and theoretical branches of modern unsteady aerodynamics are somewhat disconnected in this regard and it remains unclear where the added-mass force belongs in generalized expressions of total force.

In the seminal thesis of Noca [24], which also espouses the goal of calculating force from PIV data, added mass is only briefly mentioned. Starting from a control volume analysis, applying the principle of momentum conservation, and then applying various vector identities to remove the need for pressure information, Noca *et al.* [25] arrived at the following expression of force for impermeable bodies in unbounded incompressible fluid domains:

$$\mathbf{F} = -\frac{\rho}{N-1}\frac{d}{dt}\int_V \mathbf{x}\times\boldsymbol{\omega}\,dV - \frac{\rho}{N-1}\frac{d}{dt}\oint_{S_b}\mathbf{x}\times(\hat{n}\times\mathbf{u})dS, \tag{8}$$

where N is the dimension of the space, S_b is the surface of the body, and $\hat{n}$ is the outward facing normal on S_b (facing into the fluid). Noca [24] notes that the second integral in Eq. (8) is identically equal to the added-mass force when all of the vorticity is contained within thin boundary layers attached to the body. In the case of separated flows, the relationship between this second integral and the classical added-mass force is not explained.

Interestingly, in a 2001 conference abstract, Noca [26] claims to have derived a generalized decomposition of force into added-mass and circulatory components which is "correct and valid for any body shape in arbitrary motion." Noca [26] describes the work as a generalization of the decomposition presented by Shiels *et al.* [27], which is valid for an oscillating cylinder in a freestream flow. Unfortunately, the authors were unable to find any subsequent publications on this result.

Given the foregoing challenges and confusion regarding the application of the added-mass concept to realistic viscous flows, this paper will address the following questions.

(i) How is the added-mass force appropriately combined with the circulatory force for the generalized conditions of separated viscous flow around bodies of arbitrary shape undergoing arbitrary motion?

(ii) Is there a physical interpretation of the added-mass force which is valid in viscous separated flows?

Section II presents a generalized derivation of the added-mass and circulatory force decomposition for two- and three-dimensional geometries undergoing arbitrary motions. Section III demonstrates how well-known added-mass coefficients are recovered for the classical cases of a two-dimensional thin flat plate, a two-dimensional circular cylinder, and a three-dimensional sphere. In the special case of a two-dimensional thin flat plate, the derived force formula is shown in Sec. V to be a generalization of the unsteady airfoil theory of von Kármán and Sears [2] for arbitrary large-amplitude motions. The complete force formula is validated using a numerical simulation, performed by Wang and Eldredge [21], of a pitching plate in a freestream flow. The results of this numerical validation are presented in Sec. VII B. Section VIII recounts the insights garnered from the presented force formulation and highlights the potential utility of this particular force decomposition for experimental and theoretical purposes.

II. GENERALIZED DERIVATION OF THE ADDED-MASS AND CIRCULATORY FORCE DECOMPOSITION

The starting point for the present derivation is the infinite-domain impulse formula for impermeable bodies [25], as given in Eq. (8). For convenience, the force can be expressed in terms of total impulse $\mathbf{P}$ as

$$\mathbf{F} = -\rho\frac{d\mathbf{P}}{dt}, \tag{9}$$

which is equivalent to Eq. (8) when $\mathbf{P}$ is defined as

$$\mathbf{P} = \frac{1}{N-1}\int_V \mathbf{x}\times\boldsymbol{\omega}\,dV + \frac{1}{N-1}\oint_{S_b}\mathbf{x}\times(\hat{n}\times\mathbf{u})dS. \tag{10}$$

The body surface S_b must be piecewise smooth to ensure the validity of the identities used to relate volume integrals to surface integrals and vice versa [28].

Equation (10) has the advantage of being independent of the choice of origin. Noca [24] discusses the practical utility of this origin invariance, demonstrating how the origin can be set so as to minimize uncertainty propagation. In the present work, the origin will always be taken to lie at the instantaneous centroid of the body. This choice simplifies the resulting expressions while having no effect on the value of $\mathbf{P}$.

To proceed, the surface integral in Eq. (10) can be treated in one of two ways: (i) $\mathbf{u}$ can be split into irrotational and rotational components via a Helmholtz decomposition [29] or (ii) the no-slip condition can be invoked, setting $\mathbf{u}$ equal to the surface velocity $\mathbf{u_s}$. Using approach (i), nothing is assumed regarding the tangential velocity at the surface and the result is valid even in cases where the no-slip condition does not hold, e.g., potential flow models. Of course, in reality, the no-slip condition will be satisfied regardless of whether it is explicitly expressed in the mathematics. It is only using approach (i), however, that the added-mass force can be derived.

The derivation continues by mathematically extending the fluid volume into the body, which Noca refers to as the fluid-body concept. The surface integral in Eq. (8) is related to a volume integral over the body volume according to the following identity, presented by Noca [24] as the impulse-momentum identity:

$$\frac{1}{N-1}\oint_{S_b}\mathbf{x}\times(\hat{n}\times\mathbf{u})dS = \frac{1}{N-1}\int_{V_b}\mathbf{x}\times\boldsymbol{\omega}\,dV - \int_{V_b}\mathbf{u}\,dV. \tag{11}$$

The first integral on the right-hand side represents the impulse associated with the image vorticity. A suitable vorticity distribution within the body volume V_b must be found to maintain the impermeable boundary condition at the surface S_b. Saffman [6] notes that this image-vorticity distribution is not unique, but any valid image-vorticity system will give rise to the same resultant force. A Helmholtz decomposition is now applied to $\mathbf{u}$ such that

$$\mathbf{u} = \nabla\phi + \nabla\times\boldsymbol{\psi}, \tag{12}$$

where ϕ and $\boldsymbol{\psi}$ are referred to as the scalar and vector potentials, respectively. The velocity in a body-fixed frame of reference $\mathbf{u}'$ can be expressed as

$$\mathbf{u}' = \mathbf{u} - \mathbf{u}_c - \boldsymbol{\Omega}\times\mathbf{x}, \tag{13}$$

where $\boldsymbol{\Omega}$ is the angular velocity of the body and $\mathbf{u}_c$ is the instantaneous linear velocity of the body centroid. Combining Eqs. (12) and (13), one arrives at

$$\mathbf{u}' = \nabla\phi - \mathbf{u}_c + \nabla\times\boldsymbol{\psi} - \boldsymbol{\Omega}\times\mathbf{x}. \tag{14}$$

The vectors $\mathbf{u}_c$ and $\boldsymbol{\Omega}\times\mathbf{x}$ can be incorporated into the scalar and vector potentials to yield modified potentials ϕ' and $\boldsymbol{\psi}'$, which express the velocity field as observed in a body-fixed frame of reference:

$$\mathbf{u}' = \nabla\phi' + \nabla\times\boldsymbol{\psi}'. \tag{15}$$

The total impulse can now be expressed as

$$\begin{aligned}\mathbf{P} = {} & \frac{1}{N-1}\int_V \mathbf{x}\times\boldsymbol{\omega}\,dV + \frac{1}{N-1}\int_{V_b}\mathbf{x}\times\boldsymbol{\omega}\,dV - \int_{V_b}\nabla\phi' dV - \int_{V_b}\mathbf{u}_c dV \\ & - \int_{V_b}\nabla\times\boldsymbol{\psi}' dV - \int_{V_b}\boldsymbol{\Omega}\times\mathbf{x}\,dV.\end{aligned} \tag{16}$$

Since the vector $\mathbf{\Omega}$ is independent of position, the last integral in Eq. (16) simplifies to

$$\int_{V_b} \mathbf{\Omega} \times \mathbf{x}\, dV = \mathbf{\Omega} \times \int_{V_b} \mathbf{x}\, dV = 0, \tag{17}$$

where the integral of $\mathbf{x}$ vanishes because it represents the body centroid, which lies at $\mathbf{x} = 0$ by our choice of origin.

The impermeable boundary condition demands that $(\nabla \times \boldsymbol{\psi}') \cdot \hat{n} = 0$ everywhere on S_b, from which it can be shown that the penultimate integral of Eq. (16) also vanishes:

$$\int_{V_b} \nabla \times \boldsymbol{\psi}' dV = 0. \tag{18}$$

A proof of this statement is provided in Appendix A.

Since $\mathbf{u}_c$ is independent of position, the antepenultimate integral of Eq. (16) simplifies to

$$\int_{V_b} \mathbf{u}_c dV = \mathbf{u}_c V_b. \tag{19}$$

The integral involving the scalar potential can expressed in the more convenient form [24]

$$\int_{V_b} \nabla \phi' dV = \oint_{S_b} \hat{n} \phi' dS. \tag{20}$$

Equation (16) thus reduces to

$$\mathbf{P} = \frac{1}{N-1}\left[\int_V \mathbf{x} \times \boldsymbol{\omega}\, dV + \int_{V_b} \mathbf{x} \times \boldsymbol{\omega}\, dV\right] - \oint_{S_b} \hat{n}\phi' dS - \mathbf{u}_c V_b. \tag{21}$$

The first two integrals on the right-hand side of Eq. (21) will be referred to jointly as the total vortical impulse or individually as the shed-vorticity impulse $\mathbf{P}_v$ and the image-vorticity impulse $\mathbf{P}_i$, respectively. The third integral will be referred to as the potential impulse $\mathbf{P}_\phi$ and the remaining term as the body-volume impulse $\mathbf{P}_b$, yielding

$$\mathbf{P} = \mathbf{P}_v + \mathbf{P}_i + \mathbf{P}_\phi + \mathbf{P}_b. \tag{22}$$

Note that, in contrast to the decomposition of Lighthill [7], the shed-vorticity impulse term includes all of the vorticity in the fluid domain V, right up to the body surface S_b; there is no need to distinguish between Lighthill's additional vorticity and a vortex sheet fixed to the body. The total circulatory force $\mathbf{F}_c$ is related to the time derivative of the total vortical impulse according to

$$\mathbf{F}_c = -\rho \frac{d}{dt}(\mathbf{P}_v + \mathbf{P}_i) \tag{23}$$

and the added-mass force $\mathbf{F}_{am}$ arises from the time derivative of the remaining two impulse terms

$$\mathbf{F}_{am} = -\rho \frac{d}{dt}(\mathbf{P}_\phi + \mathbf{P}_b). \tag{24}$$

Returning to Eq. (10), if we take approach (ii) and enforce the no-slip condition by setting $\mathbf{u}_s = \mathbf{u}_c + \mathbf{\Omega} \times \mathbf{x}$ on S_b, the second integral on the right-hand side of Eq. (10) can be manipulated using Eq. (11) to yield

$$\frac{1}{N-1}\oint_{S_b} \mathbf{x} \times (\hat{n} \times \mathbf{u}_s) dS = -\int_{V_b} (\mathbf{u}_c + \mathbf{\Omega} \times \mathbf{x}) dV + \frac{1}{N-1}\int_{V_b} \mathbf{x} \times [\nabla \times (\mathbf{u}_c + \mathbf{\Omega} \times \mathbf{x})] dV. \tag{25}$$

Using $\nabla \times \mathbf{u}_c \equiv 0$ and $\nabla \times (\boldsymbol{\Omega} \times \mathbf{x}) \equiv 2\boldsymbol{\Omega}$ and manipulating the first integral on the right-hand side of Eq. (25) as before, we arrive at

$$\mathbf{P} = \frac{1}{N-1}\int_V \mathbf{x} \times \boldsymbol{\omega}\, dV - \mathbf{u}_c V_b + \frac{1}{N-1}\int_{V_b} \mathbf{x}\, dV \times 2\boldsymbol{\Omega}. \tag{26}$$

By Eq. (17), the last integral vanishes to yield

$$\mathbf{P} = \frac{1}{N-1}\int_V \mathbf{x} \times \boldsymbol{\omega}\, dV - \mathbf{u}_c V_b. \tag{27}$$

Using the previously established definitions in Eqs. (21) and (22), the total impulse can be expressed as

$$\mathbf{P} = \mathbf{P}_v + \mathbf{P}_b, \tag{28}$$

which is equivalent to the formulation given by Wu [5]. Equations (22) and (28) will hereafter be referred to as the added-mass formulation (formulation 1) and the no-slip formulation (formulation 2), respectively. These formulations must be identical for any flow in which the no-slip condition is physically satisfied; therefore,

$$\mathbf{P}_i + \mathbf{P}_\phi \equiv 0 \tag{29}$$

at all times in such cases. The implications of this relationship will be discussed further in Sec. VIII B.

III. REDERIVATION OF CLASSICAL ADDED-MASS FORCE EXPRESSIONS

The added-mass force was defined in the preceding section to be

$$\mathbf{F}_{am} = \rho \frac{d}{dt}\left(\oint_{S_b} \hat{n}\phi' dS + \mathbf{u}_c V_b \right). \tag{30}$$

Equation (30) is not a standard expression of the added-mass force. It is, however, equivalent to Saffman's [6] definition, given in Eq. (4), wherein the scalar potential represents the velocity in the absolute frame of reference. In the present section, it is demonstrated that Eq. (30) yields the well-known added-mass force expressions for the canonical cases of a two-dimensional circular cylinder, a two-dimensional thin flat plate, and a three-dimensional sphere. These general derivations emphasize two noteworthy points: (i) For bodies of nonzero volume, acceleration of the freestream relative to the body generates more force than the same relative acceleration of the body in a steady freestream and (ii) the general expression of the added-mass force for a thin flat plate includes a tangential component.

A. Two-dimensional circular cylinder

The scalar potential is the solution to the Laplace equation

$$\nabla^2 \phi' = 0 \tag{31}$$

in the fluid domain V, subject to the boundary conditions

$$\nabla \phi' = \mathbf{U}_\infty - \mathbf{u}_c \quad \text{at infinity}, \tag{32}$$

$$\nabla \phi' \cdot \hat{n} = 0 \quad \text{on } S_b. \tag{33}$$

Since Eq. (31) is linear, we can express ϕ' as the sum of two independent potentials

$$\phi' = \phi'_\infty + \phi'_c, \tag{34}$$

where ϕ'_∞ and ϕ'_c are the potential fields associated with the freestream velocity (in the absolute frame of reference) and the velocity of the body itself, respectively. These potentials both satisfy the

Laplace equation and they are both subject to the boundary condition on S_b given in Eq. (33), but they are subject to differing boundary conditions at infinity,

$$\nabla\phi_c' = -\mathbf{u}_c \quad \text{at infinity}, \tag{35}$$

$$\nabla\phi_\infty' = \mathbf{U}_\infty \quad \text{at infinity}, \tag{36}$$

such that the sum of the two potentials satisfies Eq. (32) at infinity.

Consider a circular cylinder of radius a. The solutions ϕ_c' and ϕ_∞' both take the form of ϕ_n [8],

$$\phi_n(r,\theta) = U\left(r + \frac{a^2}{r}\right)\cos\theta, \tag{37}$$

where r is the radial position vector from the center of the cylinder and U is the magnitude of the far-field velocity for the potential of interest. Here θ is measured counterclockwise from the direction U, which will be denoted by the unit vector $\hat{u}_1$. We set $r = a$ on the surface S_b and the potential on S_b becomes

$$\phi_n(a,\theta) = 2aU\cos\theta. \tag{38}$$

The surface normal can be expressed as

$$\hat{n} = \hat{u}_1\cos\theta + \hat{u}_2\sin\theta, \tag{39}$$

where $\hat{u}_2$ is oriented 90° counterclockwise from $\hat{u}_1$. The potential impulse integral for ϕ_n becomes

$$\oint_{S_b} \hat{n}\phi_n(a,\theta)dS = 2a^2U\left[\hat{u}_1\int_0^{2\pi}\cos^2\theta\,d\theta + \hat{u}_2\int_0^{2\pi}\sin\theta\cos\theta\,d\theta\right] \tag{40}$$

$$= 2\pi a^2U\hat{u}_1. \tag{41}$$

The complete potential impulse is the sum of the impulse associated with ϕ_c' and ϕ_∞', yielding

$$\mathbf{P}_\phi = -2\pi a^2(\mathbf{U}_\infty - \mathbf{u}_c). \tag{42}$$

The body-volume impulse is

$$\mathbf{P}_b = -\pi a^2\mathbf{u}_c. \tag{43}$$

The total added mass force, as defined in Eq. (30), thus becomes

$$\mathbf{F}_{am} = 2\rho\pi a^2\left(\frac{d\mathbf{U}_\infty}{dt}\right) - \rho\pi a^2\left(\frac{d\mathbf{u}_c}{dt}\right). \tag{44}$$

When the freestream flow is steady and the body accelerates, this equation yields the well-known added-mass force for a linearly accelerating cylinder. However, for the same relative acceleration between the freestream flow and the cylinder, twice the force is generated if the fluid is accelerated rather than the body (as observed from an inertial frame of reference). Within the marine literature, this is a well-known result (see, e.g., [4,7]). The excess force generated by the acceleration of the freestream, as compared to an equivalent acceleration of the body, is known as the Froude-Krylov force [7].

Since the velocity derivatives in Eq. (44) are vector derivatives, the added-mass force need not be aligned with the instantaneous velocity relative to the body. For example, for an orbiting cylinder, a centripetal acceleration produces a component of $d\mathbf{u}_c/dt$ which is perpendicular to $\mathbf{u}_c$.

In the case of a cylinder oscillating transversely to a steady freestream flow, the added-mass force is always aligned in direct opposition to the instantaneous linear acceleration of the cylinder and its form is identical to the classical added-mass formulation. This result stands in contrast to the recent proposal by Konstantinidis [30] of a more complicated added-mass force expression for the

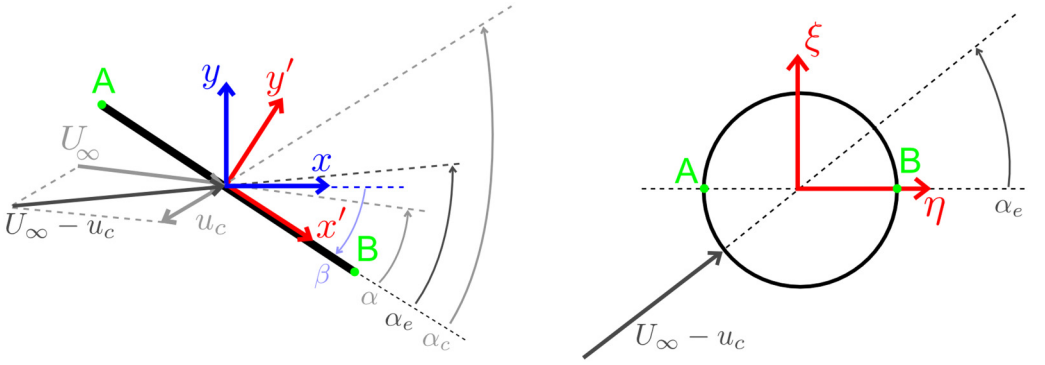

(a) (b)

FIG. 1. (a) Plate-fixed and plate-centered coordinate systems. (b) Coordinate system in the circle domain, related to the plate-fixed frame of reference via the conformal map given in Eq. (47). Point A in the plate domain maps to point A in the circle domain and the points labeled B likewise map to one another. All angles are treated as counterclockwise positive.

oscillating cylinder case. Since Eq. (30) is generally superimposable onto the circulatory force, such additional complexity seems to be avoidable.

B. Two-dimensional thin flat plate

For a two-dimensional plate of infinitesimal thickness, the body volume is zero such that $\mathbf{P}_b = 0$ and the added-mass force arises from the time derivative of the potential impulse alone. The potential flow around a flat plate can be solved through a conformal map relating the fluid domain around the flat plate to that around a cylinder. The solution for the scalar potential around a cylinder is already known [Eq. (37)] and we take advantage of the fact that the scalar potential is invariant to conformal transformations [31]. Let x' and y' be orthogonal basis vectors in the plate domain, oriented in alignment with and perpendicular to the plate, respectively. Further, η and ξ are the corresponding basis vectors in the circle domain (see Fig. 1). The complex position variables are defined as

$$z' = x' + iy', \tag{45}$$

$$\zeta = \eta + i\xi, \tag{46}$$

where $i = \sqrt{-1}$. The conformal map relating these two variables is given as

$$z'(\zeta) = \zeta + \frac{a^2}{\zeta}, \tag{47}$$

where a is radius of the cylinder. As $\zeta \to \infty, z \to \zeta$ such that the conformal map has no effect on the boundary condition at infinity. The boundary condition on the solid boundary remains $\nabla\phi' \cdot \hat{n} = 0$ in both domains. In the circle domain, the boundary is defined by the curve

$$\zeta = ae^{i\theta} \quad \text{on } S_b, \tag{48}$$

where θ is measured from the η axis and defined as positive counterclockwise. The cylinder surface maps directly to the plate surface such that

$$z' = 2a\cos\theta \quad \text{on } S_b. \tag{49}$$

Noting that $\theta = \{0,\pi\}$ maps to $z = \{c/2,-c/2\}$, where c is the plate chord, it is clear that $a = c/4$ and the relationship $z' = z'(\theta)$ becomes

$$z'(\theta) = \frac{c}{2}\cos\theta \quad \text{on } S_b. \tag{50}$$

The scalar potential on the surface of the circle is also expressed as a function of θ, modified from Eq. (38) to account for the effective angle of incidence α_e,

$$\phi'(\theta) = \tfrac{1}{2}cU\cos(\theta - \alpha_e), \tag{51}$$

where α_e is measured from the η axis to the direction of the effective incident velocity and is defined as positive counterclockwise. The effective angle of incidence in the plate domain, measured relative to the x' axis, is unaffected by the conformal transformation. Here U is the magnitude of the fluid velocity relative to the body at infinity, given as

$$U = |\mathbf{U}_\infty - \mathbf{u}_c|. \tag{52}$$

Although the scalar potential is transformation invariant, the potential impulse is not. After a change of variable, the potential impulse in the plate domain becomes

$$\mathbf{P}_\phi = -\hat{y}'\frac{c}{2}\int_0^{2\pi}\phi'(\theta)\sin\theta\, d\theta \tag{53}$$

$$= -\hat{y}'U\frac{c^2}{4}\int_0^{2\pi}\cos(\theta-\alpha_e)\sin\theta\, d\theta \tag{54}$$

$$= -\left[\left(\frac{\pi c^2}{4}\right)U\sin\alpha_e\right]\hat{y}', \tag{55}$$

where $\hat{y}'$ is the plate-normal unit vector of unchanging sign. Equation (55) can also be written as

$$\mathbf{P}_\phi = -\left(\frac{\pi c^2}{4}\right)\mathbf{U}_\perp \tag{56}$$

$$= -\left(\frac{\pi c^2}{4}\right)(U_\infty\sin\alpha - u_c\sin\alpha_c)\hat{y}', \tag{57}$$

where $\mathbf{U}_\perp$ is the normal component of the far-field velocity as viewed in the plate-fixed frame of reference. Here α and α_c represent the angles, measured counterclockwise positive, from the x' axis to the vectors $\mathbf{U}_\infty$ and $-\mathbf{u}_c$, respectively (see Fig. 1). It must be noted that $\hat{y}'$ is not constant under rotations of the plate and its derivative is equal to

$$\frac{d\hat{y}'}{dt} = \boldsymbol{\Omega}\times\hat{y}' = -\Omega\hat{x}', \tag{58}$$

where $\hat{x}'$ is the tangential unit vector and a positive Ω represents counterclockwise rotation of the plate. The added-mass force therefore includes both a normal and a tangential component

$$\mathbf{F}_{am} = \frac{\rho\pi c^2}{4}\left[\left(\sin\alpha\frac{dU_\infty}{dt} + U_\infty\cos\alpha\frac{d\alpha}{dt}\right)\hat{y}' - (U_\infty\Omega\sin\alpha)\hat{x}'\right.$$
$$\left. -\left(\sin\alpha_c\frac{du_c}{dt} + u_c\cos\alpha_c\frac{d\alpha_c}{dt}\right)\hat{y}' + (u_c\Omega\sin\alpha_c)\hat{x}'\right]. \tag{59}$$

The added-mass force expression presented by Polet *et al.* [23], which generalizes Theodorsen's result for large angles, is a special case of Eq. (59). They considered a flat plate which rotates about a fixed pivot point lying on the chord line, while this pivot point linearly accelerates in a quiescent

fluid. Taking the normal component of Eq. (59), setting $U_\infty = 0$ and $dU_\infty/dt = 0$, and normalizing to yield the added-mass force coefficient C_{am}, the equation reduces to

$$C_{am} = \frac{\mathbf{F}_{am} \cdot \hat{y}'}{1/2\rho c U_0^2} = \frac{\pi c}{2U_0^2}\left[-\sin\alpha_c \frac{du_c}{dt} + u_c \cos\alpha_c \frac{d\alpha_c}{dt}\right], \tag{60}$$

where U_0 is a characteristic velocity. After a change of notation, Eq. (60) can be shown to be equivalent to Eq. (2.4) in the work of Polet *et al.* [23] (N.B. u_c refers to the plate centroid velocity, whereas the velocity of the pivot point is treated in [23]).

The tangential component of the added-mass force is nonintuitive, as one expects a purely normal force in the absence of viscosity or circulation. However, no physical contradiction is implied; the total force can remain plate normal so long as the vorticity field evolves to yield a circulatory force which cancels this tangential component of the added-mass force.

C. Axisymmetric flow over a sphere

The scalar potential associated with the irrotational velocity field around a sphere in a body-fixed frame of reference is expressed as [8]

$$\phi_m = U\cos\theta\left[r + \frac{a^3}{2r^2}\right], \tag{61}$$

where r is the radial distance from the center of the sphere, a is the radius of the sphere, U is the far-field velocity relative to the body, and θ is the angular coordinate measured relative to the direction of U. As with the two-dimensional cases, the scalar potential ϕ_m is a solution to Eq. (31) that satisfies the boundary conditions in Eqs. (32) and (33).

The velocity field is axisymmetric about the flow direction, so the scalar potential has no dependence on the azimuthal angle λ. On the surface of the body, $r = a$ and the potential impulse associated with this flow field is calculated as

$$-\oint_{S_b} \hat{n}\phi_m dS = -\int_0^{\pi}\int_0^{2\pi} \hat{n}\left(\frac{3}{2}Ua\cos\theta\right)\sin\theta\, a^2 d\lambda\, d\theta. \tag{62}$$

The unit normal $\hat{n}$ is the only variable with dependence on λ such that

$$-\oint_{S_b} \hat{n}\phi_m dS = -\frac{3}{2}a^3 U\int_0^{\pi}\left[\int_0^{2\pi}\hat{n}d\lambda\right]\cos\theta\sin\theta\, d\theta. \tag{63}$$

The λ integral, evaluated over a circular cross section of the sphere at constant θ, is evaluated as

$$\int_0^{2\pi}\hat{n}d\lambda = 2\pi\cos\theta\,\hat{u}_1, \tag{64}$$

where $\hat{u}_1$ is the unit vector in the direction of U. The θ integral to be evaluated thus becomes

$$\int_0^{\pi}\cos^2\theta\sin\theta\, d\theta = \frac{2}{3} \tag{65}$$

and Eqs. (62)–(64) combine to yield

$$-\oint_{S_b}\hat{n}\phi_m dS = -2\pi a^3 U\hat{u}_1. \tag{66}$$

The potential impulse for the sphere is therefore

$$\mathbf{P}_\phi = -2\pi a^3(\mathbf{U}_\infty - \mathbf{u}_c), \tag{67}$$

the body-volume impulse is

$$\mathbf{P}_b = -\tfrac{4}{3}\pi a^3\mathbf{u}_c, \tag{68}$$

and the added-mass force acting on the sphere is

$$\mathbf{F}_{am} = 2\pi\rho a^3 \left[\frac{d\mathbf{U}_\infty}{dt} - \frac{1}{3}\frac{d\mathbf{u}_c}{dt} \right]. \tag{69}$$

When a sphere accelerates in a steady freestream flow, this equation reduces to the added-mass force given in the literature for an accelerating sphere in quiescent fluid (see, e.g., [8]). If instead the freestream accelerates relative to a nonaccelerating sphere, the generated force is greater by a factor of 3. This factor is geometry dependent and may only be assumed to be unity for bodies of zero volume (recall that a factor of 2 was found previously for the two-dimensional circular cylinder).

IV. IMAGE-VORTICITY IMPULSE FOR A TWO-DIMENSIONAL THIN FLAT PLATE

The derivation in Sec. II clearly demonstrates that the potential impulse, which contributes to the added-mass force, arises in conjunction with the image-vorticity impulse. In order to appropriately use the added-mass force in an aerodynamic model or during the calculation of force from well-resolved vorticity-field data, each vortical fluid element in the fluid domain must have an appropriate image with associated impulse. In the present section, a convenient expression of image-vorticity impulse for a thin flat plate is derived. Complex notation is used, as the derivation relies on conformal mapping techniques. The resulting expression cannot be easily converted into vector notation, so it is with some regret that the authors switch notation for the remainder of this paper.

The impermeable boundary condition on the plate is usually associated with a distribution of sheet vorticity on the chord line $\gamma = \gamma(x')$, where the velocity induced by γ exactly cancels the sum of the freestream velocity and the induced velocity of the shed vorticity along the chord. For a given circulation about the plate, a unique distribution $\gamma(x')$ can be determined in a number of ways (see, e.g., [2,22,32]) and the total impulse is expressed as

$$\mathbf{P} = \int_V \mathbf{x} \times \boldsymbol{\omega}\, dV + \hat{y}' \int_{-c/2}^{c/2} x'\gamma(x')dx', \tag{70}$$

where the last integral on the right-hand side represents the potential impulse and the image-vorticity impulse combined. In complex notation, defining $z = x + iy$, the total impulse can be expressed as

$$P = P_x + iP_y \tag{71}$$

$$= -i\int_V z\omega\, dV - ie^{i\beta}\int_{-c/2}^{c/2} x'\gamma(x')dx', \tag{72}$$

where β is the angle from the x axis to the x' axis, measured counterclockwise positive.

In the present work, we are concerned only with the dynamic effect of the image vorticity, not with its kinematic effect on the velocity field. We therefore avoid explicitly solving for the sheet-vorticity distribution. To do so, we require the following theorem.

Theorem. For an unbounded, two-dimensional fluid domain, the total vortical impulse is invariant to a conformal transformation which has no effect at infinity.

That is, if we choose a map $z = z(\zeta)$ such that as $\zeta \to \infty$, $z \to \zeta$, then the total vortical impulse calculated in the two domains will be equal. A proof of this statement is provided in Appendix B. The proof does not seem to require the flow to be irrotational at infinity, but only such cases are considered in the present work.

The derivation of total impulse presented by Wang and Eldredge [21] supports this postulate. First, the vortical impulse integrals are discretized according to

$$\int_V z\omega\, dV = \left[\sum_j z_j \Gamma_j \right]_V \tag{73}$$

such that each vortical fluid element is treated as a point vortex of circulation $\Gamma_j = \omega_j dV$. Such discretization is necessary to calculate impulse and force from discrete data sets. Then mapping the

plate domain to the unit circle domain according to

$$z = \frac{c}{4}\left(\zeta^* + \frac{1}{\zeta^*}\right)e^{i\beta}, \tag{74}$$

where ζ^* is the dimensionless complex position variable in the circle domain, Wang and Eldredge [21] arrived at an expression of total impulse for a thin flat plate which is equivalent to

$$P = ie^{i\beta}\left[-\frac{\pi c^2}{4}U_\perp - \frac{c}{4}\sum_j \Gamma_j\left(\zeta_j^* - \frac{1}{\overline{\zeta_j^*}}\right)\right], \tag{75}$$

where $\overline{\zeta_j^*}$ is the complex conjugate of ζ_j^*. By the circle theorem [33], $1/\overline{\zeta_j^*}$ is the image-vortex location corresponding to ζ_j^* for a unit circle, which is generalized to $a^2/\overline{\zeta_j^*}$ for a circle of radius a. The first term on the right-hand side represents the potential impulse and is equivalent to Eq. (57) derived in Sec. III B. The remaining terms on the right-hand side are recognizable as the total vortical impulse evaluated in the circle domain, multiplied by a constant factor owing to the chosen conformal map. We now choose the alternative map

$$z' = \zeta + \frac{1}{16}\frac{c^2}{\zeta}, \tag{76}$$

which maps the plate domain in a plate-fixed frame of reference to a circle of radius $c/4$ with no effect at infinity. Note that ζ has dimensions of length in this map. By the postulated transformal invariance of total vortical impulse, we can express the total impulse in the plate-fixed frame of reference P' as

$$P' = -i\frac{\pi c^2}{4}U_\perp - i\sum_j \Gamma_j\left(\zeta_j - \frac{c^2}{16\overline{\zeta_j}}\right), \tag{77}$$

which can be rotated to the absolute frame of reference using

$$P = e^{i\beta}P'. \tag{78}$$

For convenience, the vortical impulse can be expressed in terms of the physical coordinate z' using Eq. (76). The last term on the right-hand side of Eq. (77) can be manipulated as follows:

$$\zeta_j - \frac{c^2}{16\overline{\zeta_j}} = \left(\zeta_j + \frac{c^2}{16\zeta_j}\right) - \frac{c^2}{16}\left(\frac{1}{\zeta_j} + \frac{1}{\overline{\zeta_j}}\right) \tag{79}$$

$$= z'_j - \frac{c^2}{8}\,\mathrm{Re}\left[\frac{1}{\zeta_j}\right], \tag{80}$$

$$= c\left(z_j'^* - \frac{1}{8}\,\mathrm{Re}\left[\frac{1}{\zeta_j'^*}\right]\right), \tag{81}$$

where the operator $\mathrm{Re}[\cdot]$ returns the real component of a complex number and the asterisk superscript denotes normalization by chord length. The last term on the right-hand side can also be expressed in terms of z'^* using the inverse map. Normalizing z and ζ by chord length and rearranging Eq. (76), we obtain two possible solutions

$$\{\zeta_1^*, \zeta_2^*\} = \frac{z'^*}{2} \pm \sqrt{\left(\frac{z'^*}{2}\right)^2 - \frac{1}{16}}. \tag{82}$$

Only one of these solutions will lie on or outside the circle, i.e., in the fluid domain, and this is taken as the physically meaningful solution pertaining to any position z'^*. We select the appropriate

solution according to

$$\zeta^* = \mathrm{cmax}\{\zeta_1^*, \zeta_2^*\}, \tag{83}$$

where the operator $\mathrm{cmax}\{\cdot\}$ is defined such that it returns the complex number of greater modulus. Combining Eqs. (77) and (81)–(83) and normalizing impulse by chord length and characteristic velocity, we arrive at

$$P'^* = i\left[-\frac{\pi}{4} U_\perp^* - \sum_j \Gamma_j^* z_j'^* + \frac{1}{2} \sum_j \Gamma_j^* g(z_j'^*) \right]. \tag{84}$$

The terms on the right-hand side of Eq. (84) represent potential impulse, shed-vorticity impulse, and image-vorticity impulse, in that order. The function $g : \mathbb{C} \to \mathbb{R}$ is defined as

$$g(z'^*) = \mathrm{Re}\left[\frac{1}{\mathrm{cmax}\{2z'^* \pm \sqrt{(2z'^*)^2 - 1}\}} \right], \tag{85}$$

returning a real value between $-1/2$ and $1/2$ for any complex input argument. This value can be interpreted as the chord-normalized centroid position of the sheet-vorticity distribution induced by a shed-vortical fluid element.

V. EQUIVALENCE TO THE UNSTEADY AIRFOIL THEORY OF VON KÁRMÁN AND SEARS

von Kármán and Sears [2] presented a theory of airfoils in unsteady motion using the concept of impulse. Given their assumptions of small-amplitude motions and a planar wake, Eq. (84) reduces to their expression of impulse. Changes in notation from [2] have been made for consistency with the present paper.

von Kármán and Sears [2] express the instantaneous lift on an airfoil as the time derivative of total impulse, whose magnitude $|P|$ is

$$|P| = \int_{-c/2}^{c/2} \gamma_0(x) x \, dx + \int_{c/2}^{\infty} \gamma(x) x \, dx + \int_{c/2}^{\infty} \gamma(x) [\sqrt{x^2 - (c/2)^2} - x] dx, \tag{86}$$

where γ_0 represents the distribution of vorticity on the chord associated with the freestream velocity and body motion. The three integrals are on the right-hand side of Eq. (86) are the potential, shed-vorticity, and image-vorticity impulses, in that order. Through simple algebra, it can be shown that

$$\sqrt{x^2 - (c/2)^2} - x = -\frac{c}{2}\left(\frac{1}{2x^* + \sqrt{(2x^*)^2 - 1}} \right), \tag{87}$$

where $x^* = x/c$. The term in large parentheses on the right-hand side is equivalent to the right-hand side of Eq. (85) when one assumes that all shed-vorticity fluid elements lie on the positive x axis (real line). When the pitch amplitude is assumed to be small, it can be assumed that $P = P'$ and Eq. (84) represents a generalization of the impulse formula of von Kármán and Sears [2] which removes the planar-wake restriction. When pitch amplitudes are not small, P' can be rotated to yield P using Eq. (78), providing a general means of calculating force which is valid for any motion of the plate and any concomitant vorticity-field evolution.

VI. IMPULSE AND FORCE EXPRESSIONS FOR A TWO-DIMENSIONAL THIN FLAT PLATE IN ARBITRARY MOTION

For the specific case of a two-dimensional thin flat plate in a steady freestream flow, the impulse terms in Eq. (22) are expressed below in complex notation. Denoting the normal and tangential directions as the imaginary and real axes, respectively, we obtain

$$F' = F_t + i F_n, \tag{88}$$

where F_t and F_n are the tangential and normal forces, respectively, and the force in the absolute frame of reference is simply $F = F' e^{i\beta}$. Here F' is normalized according to

$$F'^* = \frac{F'}{\rho c U_\infty^2}. \tag{89}$$

When $\mathbf{U}_\infty$ is aligned with the positive x axis, $\beta = -\alpha$ and F'^* becomes

$$F'^* = -\frac{dP'^*}{dt^*} + iP'^* \frac{d\alpha}{dt^*}, \tag{90}$$

where $P'^* = P'/c^2 U_\infty$. The components of impulse in the plate-fixed frame of reference can then be expressed as

$$P_v'^* = i \sum_j \Gamma_j^* z_j'^*, \tag{91}$$

$$P_i'^* \approx -\frac{i}{2} \sum_j \Gamma_j^* \operatorname{Re}\left[\frac{1}{c \max\{2z'^* \pm \sqrt{(2z'^*)^2 - 1}\}} \right], \tag{92}$$

$$P_\phi'^* = -i \frac{\pi}{4} \left(\sin\alpha + \frac{1}{2} \frac{d\alpha}{dt^*} \right), \tag{93}$$

$$P_b'^* = -ib^* \left(\frac{1}{2} \frac{d\alpha}{dt^*} \right), \tag{94}$$

where $b^* = b/c$ is the normalized plate thickness, $t^* = tU_\infty/c$, and $\Gamma_j^* = \Gamma_j/cU_\infty$. The approximation in the image-vorticity impulse reflects the assumption that the plate is infinitely thin. For thin plates where this approximation is valid, Eq. (94) tends to zero as $b^* \to 0$, but it is included for completeness. Formulation 1 is thus evaluated by setting

$$P'^* = P_v'^* + P_i'^* + P_\phi'^* + P_b'^* \tag{95}$$

and formulation 2 is evaluated using

$$P'^* = P_v'^* + P_b'^*. \tag{96}$$

The tangential and normal force coefficients C_t and C_n are given as

$$C_t = 2 \operatorname{Re}(F'^*), \tag{97}$$

$$C_n = 2 \operatorname{Im}(F'^*), \tag{98}$$

where $\operatorname{Im}(\cdot)$ returns the magnitude of the imaginary component of a complex number.

VII. NUMERICAL VALIDATION

In order to validate formulations 1 and 2 as presented in Sec. VI, we make use of a numerical data set generated by Wang and Eldredge [21] and disseminated among the research community. The three key objectives of this validation are (i) to demonstrate that the force formulations can be applied accurately to discretized data, (ii) to demonstrate that the force contributions of the image-vorticity impulse and the potential impulse cancel, as predicted due to the no-slip condition, and (iii) to demonstrate that for a flat plate undergoing separation at both edges, the tangential component of added-mass force is canceled by the circulatory force to yield a dominantly normal force.

A. Methodology of Wang and Eldredge

Wang and Eldredge [21] numerically investigated a two-dimensional pitching plate, of thickness $0.023c$ with rounded edges, in a steady freestream flow. The plate was held at a zero angle of

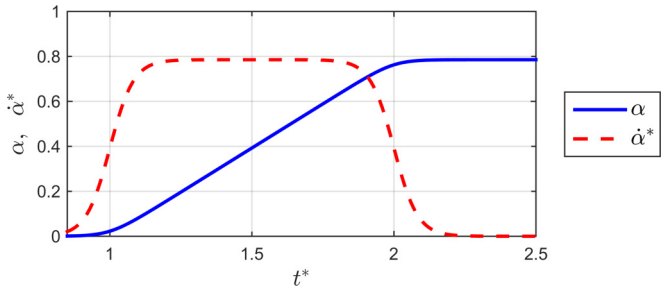

FIG. 2. Time history of the plate angle of attack α (in radians) and normalized pitch rate $\dot{\alpha}^*$ in the simulation of Wang and Eldredge [21].

attack for about one convective time (the time it takes a fluid particle to travel one chord at the freestream velocity) to allow the boundary layers to develop and then pitched about the leading edge to a maximum angle of attack of $\pi/4$ radians. The Reynolds number of the simulation was 1000. Dimensionless times from $t^* = 0.85$ to $t^* = 2.5$ are considered, where $t^* = tU_\infty/c$. The angle of attack and dimensionless pitch rate $\dot{\alpha} = \alpha c/U_\infty$ are plotted versus t^* in Fig. 2.

The numerical scheme used by Wang and Eldredge [21] to solve for the resulting flow field, known as the viscous vortex particle method, is described in detail by Eldredge [34]. Vorticity is carried through the flow field by discrete particles and viscous diffusion is accounted for through the exchange of vorticity between particles. Vorticity is generated at the surface by diffusing vorticity from the vortex sheet on the body surface, which is imposed to maintain the impermeable boundary and no-slip conditions, to neighboring particles. The results of Wang and Eldredge [21] have been shared in Eulerian form, having been interpolated onto a square grid with $0.01c$ spacing.

B. Results

A sequence of vorticity-field snapshots from the results of Wang and Eldredge [21] is shown in Fig. 3. The force coefficients are calculated from this vorticity data using Eqs. (90)–(98) in Sec. VI. These calculated force coefficients are compared to those reported by Wang and Eldredge [21] in Fig. 4. The calculated and reported tangential force coefficients show close agreement and remain near zero for the duration of the investigation. In the plate-normal direction, both force formulations show fairly good agreement with the reported force coefficients. Small discrepancies are noted during the periods of angular acceleration at the beginning and end of the pitch maneuver (around $t^* = 1$ and $t^* = 2$). A discrepancy is also noted towards the end of the constant pitch rate portion of the maneuver (from approximately $t^* = 1.4$ to 1.8). These errors could be partially attributable to numerical error in the interpolation of the Lagrangian vortex-particle data onto an Eulerian grid [25] or due to our assumption that each vorticity data point occupies the same elemental area (which is not strictly true near the body). However, it is not obvious whether these numerical effects can explain the errors entirely and further work will be required to quantify the effect of discretization on the accuracy of the force formulation.

The normal-force coefficients calculated using Eqs. (95) and (96) are in close agreement with one another, but with the output of the latter exhibiting a spurious oscillatory component superimposed onto the trend of the former. It is believed that this spurious component, hereafter referred to as noise for simplicity, is due to the spatial discretization of the data. As the plate rotates through the square grid, locations which begin under the plate then pass through the plate (where vorticity is zero) and finally emerge above the plate. These discrete changes in vorticity, and associated impulse, could lead to oscillations in the calculated force. Moreover, if one coarsens the grid by using only every second data point, the amplitude of the noise increases, indicating its relationship to spatial discretization. It is speculated that this noise is reduced using formulation 1 due to the cancellation

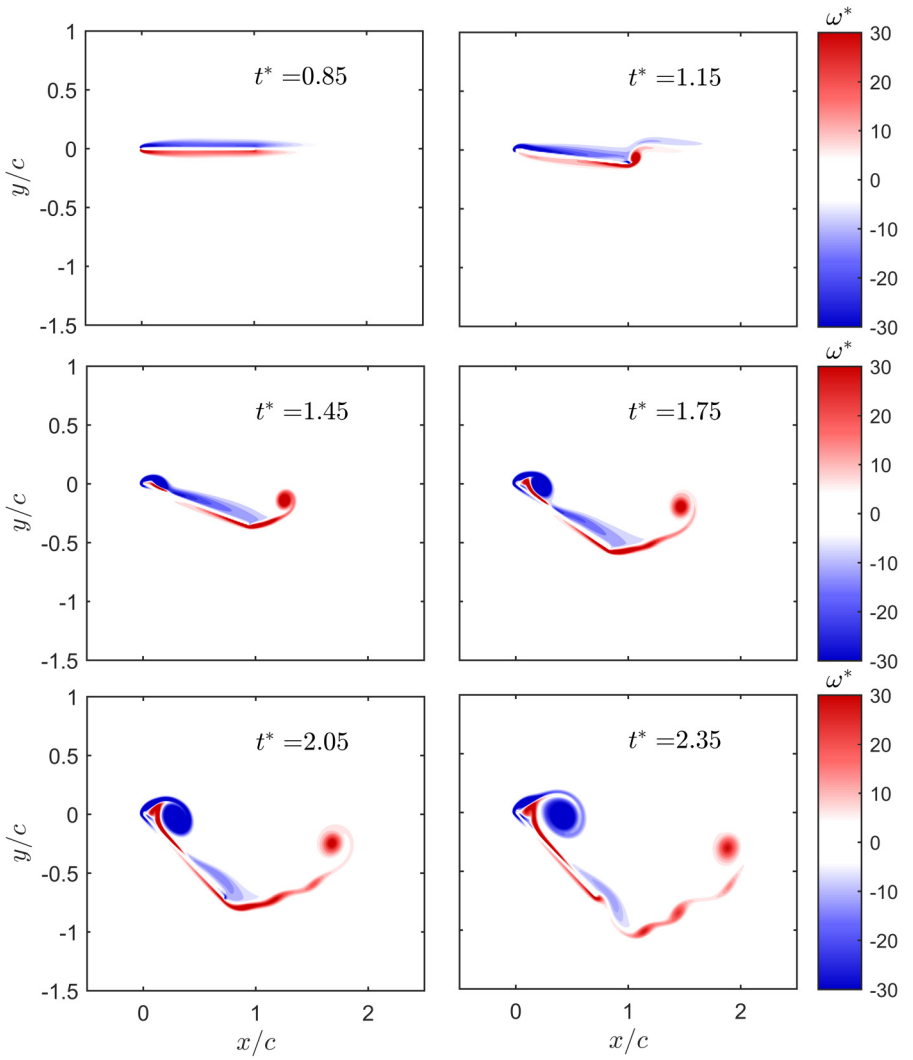

FIG. 3. Normalized vorticity plots at discrete times during the pitch maneuver from $\alpha = 0$ to $\pi/4$ rad. The freestream velocity is from left to right.

between the shed-vorticity and image-vorticity impulse terms near the body, whereby numerical errors are introduced into each term with opposite signs. This cancellation is discussed further in Sec. VIII A below.

The contributions of the various impulse terms to the total normal force are demonstrated in Figs. 5(a) and 5(b). The subscripts v, i, ϕ, and b represent the contributions of the shed-vorticity, image-vorticity, potential, and body-volume impulse terms, respectively. The variable $C_{n,v}$, for example, represents the contribution of the shed-vorticity impulse to the plate-normal force. The noise in the shed-vorticity impulse contribution to normal force is qualitatively similar to that in the image-vorticity impulse contribution; in Eq. (95), the sum of the two signals yields the smoother force history seen in Fig. 4 for formulation 1.

As predicted in Eq. (29), the potential and image-vorticity terms are of equal and opposite magnitude for all times due to the no-slip condition. In Fig. 5(b), the potential impulse is seen to lend a nonzero contribution to the tangential force which is canceled by the image-vorticity impulse

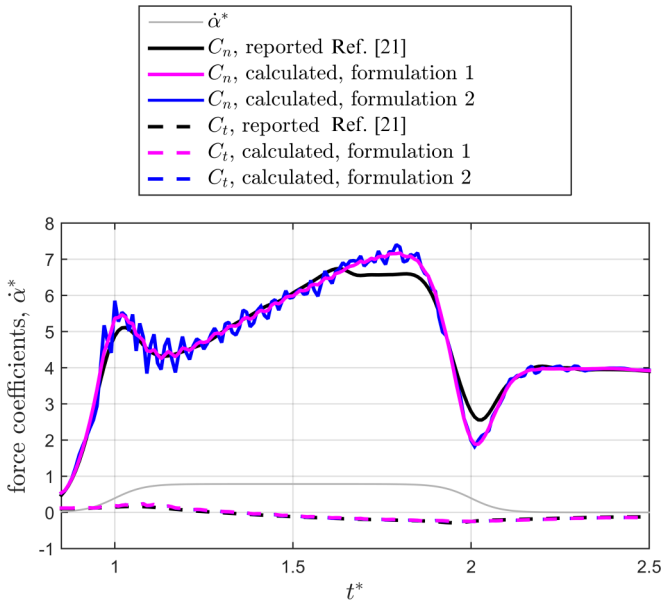

FIG. 4. Comparison of force coefficients calculated from the vorticity field using formulation 1 [the added-mass formulation (95)] and formulation 2 [the no-slip formulation (96)] with the force coefficients reported by Wang and Eldredge [21].

term to yield a near-zero force, as expected for a plate experiencing flow separation at both edges at a Reynolds number $\mathrm{Re} \sim O(10^3)$. In Fig. 5(a), this cancellation is also observed in the plate-normal direction, neglecting the noise in the image-vorticity contribution.

VIII. DISCUSSION

A. Physical interpretation of added mass

As discussed briefly in Sec. I, a common physical interpretation of added mass is that it arises due to the acceleration of near-body fluid. This interpretation is not justified given its derivation from the irrotational flow assumption. Herein, we advocate for the alternative view in which added mass is related to near-body vorticity, in agreement with discussions found in the work of Lighthill [7], Noca [24], and Wu *et al.* [12] (p. 304).

An association between added mass and vorticity has long been acknowledged. In classical thin-airfoil theory, the added-mass force can be expressed in terms of the vortical impulse of a distribution of sheet vorticity along the chord [2], as shown in Eq. (86). This association extends to bodies of arbitrary geometry; using the notation of the present work, Noca's discussion to that effect [24] can be summarized as follows.

When all of the vorticity is contained in a thin boundary layer attached to the body, it can be shown that $\mathbf{P}_v = \mathbf{P}_\phi$, and both force formulations presented herein will yield the expected added-mass force. For this to be true, inspection of Eqs. (22) and (28) makes it clear that $\mathbf{P}_v + \mathbf{P}_i = 0$ must also hold for the attached flow case. As the flow separates, the relationships $\mathbf{P}_v = \mathbf{P}_\phi$ and $\mathbf{P}_v + \mathbf{P}_i = 0$ do not hold, but the relationship between the vortical impulse and the potential impulse can be generalized.

When one applies Eq. (28) to calculate force, all of the dynamic information regarding the wake is captured in the $\mathbf{P}_v$ term. Conversely, when Eq. (22) is used, the image-vorticity impulse partially cancels the shed-vorticity impulse term and the difference is instead included in the $\mathbf{P}_\phi$ term. The cancellation between the image- and shed-vorticity impulse terms occurs mainly in the near-body region, which will be made clear below. The potential impulse can thus be said to account for the

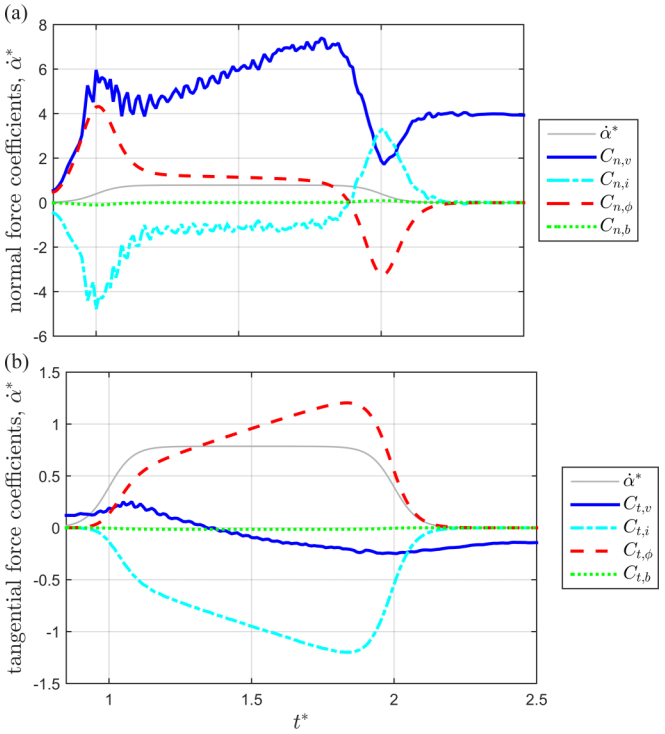

FIG. 5. Contributions of individual impulse terms to the (a) plate-normal and (b) plate-aligned force coefficients. The contribution of the shed-vorticity impulse closely follows the force coefficients reported by Wang and Eldredge [21], as shown in Fig. 4. Note the change in the vertical scale between (a) and (b).

impulse of this near-body vorticity in a manner whose calculation is independent of the vorticity field.

Noting that there are infinitely many valid image-vorticity distributions which satisfy the impermeable boundary condition [6], we can choose to express the image vorticity induced by a shed-vorticity fluid element of circulation Γ as a sheet-vorticity distribution

$$\boldsymbol{\gamma} = \boldsymbol{\gamma}(\mathbf{x}_s), \tag{99}$$

where $\mathbf{x}_s \in S_b$. As the vortical fluid element approaches a point $\mathbf{x}_{s1}$ on S_b, the image vorticity distribution can be expressed as

$$\boldsymbol{\gamma}(\mathbf{x}_s) = \boldsymbol{\gamma}_v \delta(\mathbf{x}_s - \mathbf{x}_{s1}), \tag{100}$$

where δ is the Dirac delta function and $\boldsymbol{\gamma}_v dS = -\Gamma$. In this way, we have effectively superimposed two point vortices of equal and opposite circulation at $\mathbf{x}_{s1}$ such that their net induced velocity everywhere is zero. Although this seems to be a trivial solution, Saffman [6] assures us that any image-vorticity distribution which satisfies the impermeable boundary condition will give rise to the same force. In terms of impulse, the image-vorticity impulse is thus evaluated as

$$\mathbf{P}_i = \frac{1}{N-1} \oint_{S_b} \mathbf{x}_s \times \boldsymbol{\gamma}\, dS \tag{101}$$

$$= -\frac{1}{N-1} \mathbf{x}_{s1} \times \Gamma, \tag{102}$$

which exactly cancels the shed-vorticity impulse, removing any dependence on the arbitrarily defined $\mathbf{x}_{s1}$.

To reiterate, as a vortical fluid element approaches the body, its associated total vortical impulse approaches zero in a continuous fashion, with the aforementioned cancellation between $\mathbf{P}_i$ and $\mathbf{P}_v$ at the surface. The importance of near-body vorticity data to the calculation of total impulse is thus reduced and the residual impulse is neatly accounted for in the potential impulse term. In cases where significant uncertainty exists in near-body vorticity data, as expected in PIV investigations, formulation 1 may therefore yield more accurate force calculations than formulation 2.

Using this vortical interpretation of the added-mass force, we can predict that it will dominate the total force expression when the near-body vorticity distribution changes more rapidly than the shed vorticity in the wake evolves. Thus, regardless of the surrounding distribution of vorticity, the added-mass force alone can yield accurate predictions of total force under sufficiently rapid rotations or sufficiently rapid linear accelerations, in agreement with experimental observations (see, e.g., [23,35]).

B. Conservation of image-vorticity impulse

At the end of Sec. II, it was noted that by the equivalence of Eqs. (22) and (28) when the no-slip condition holds, the image-vorticity impulse and potential impulse terms must exactly cancel at all times, i.e., $\mathbf{P}_i \equiv -\mathbf{P}_\phi$, which was observed in the numerical data set used for validation (see Sec. VII B). We refer to this cancellation as the conservation of image-vorticity impulse, reflecting that the image-vorticity impulse remains constant for a nonaccelerating body.

Without prior knowledge of the flow-field, we can calculate $\mathbf{P}_\phi = \mathbf{P}_\phi(t)$ from the geometry and body-motion alone; we then immediately know $\mathbf{P}_i(t)$ for all time. By the geometry-dependent relationship between image vorticity and shed vorticity, we thus have a restriction on the evolution of the vorticity field, in an integral sense, which is determined *a priori*. Incorporation of this principle into low-order aerodynamic models may be an effective way to account for the dynamic consequences of the no-slip condition.

C. Equivalence to Lighthill's force decomposition

Equation (7) presents the force decomposition proposed by Lighthill [7]. This equation can be shown to be equivalent to the force decomposition derived herein once one considers the absence of image vorticity in Lighthill's formulation and the peculiar concept of additional vorticity.

The volume integral in Eq. (7) includes only the vorticity after a vortex sheet on S_b has been subtracted from the complete physical vorticity distribution in V. Specifically, this is the vortex sheet associated with the tangential slip velocity on S_b in the presence of an acyclic potential flow. Using the terminology of the present work, one acquires an expression for the potential impulse when this vortex sheet is integrated around S_b. Thus, if we define the volume integral to include all vorticity in V, which is simply the definition of shed-vorticity impulse in three dimensions, then Lighthill's equation becomes

$$\mathbf{F} = -\rho \frac{d}{dt}[\mathbf{P}_v - \mathbf{P}_\phi] + \mathbf{M}_{ij}\dot{\mathbf{U}}. \tag{103}$$

The last term represents the classical added-mass force, which can be replaced by Eq. (24) to yield

$$\mathbf{F} = -\rho \frac{d}{dt}[\mathbf{P}_v - \mathbf{P}_\phi + \mathbf{P}_\phi + \mathbf{P}_b]. \tag{104}$$

The two $\mathbf{P}_\phi$ terms can be taken to cancel, yielding the no-slip formulation. Alternatively, one can invoke the conservation of image-vorticity impulse, as discussed above, and substitute $\mathbf{P}_i = -\mathbf{P}_\phi$ to yield the added-mass formulation. Thus, the volume integral in Lighthill's equation can be reinterpreted as the total vortical impulse, where the vortex sheet to be subtracted in Lighthill's methodology represents the image vorticity that is otherwise absent from his formulation.

D. Body-displacement force

The body-displacement force arises as the time derivative of the body-volume impulse. It results in a force that is aligned with the instantaneous linear acceleration of the body centroid in the *same* direction, i.e.,

$$\mathbf{F}_b = \rho \frac{d\mathbf{P}_b}{dt} = \rho \frac{d}{dt}(V_b \mathbf{u}_c). \tag{105}$$

One might be tempted to add a negative sign to this relation in order to yield a force that opposes the body acceleration, as physical intuition would suggest. This would be incorrect. This component of the total force can be found in the work of Wu [5], Eldredge [34], and Kriegseis and Rival [36] with the correct sign. Despite the nonintuitive nature of this force term, it never exists in isolation and therefore cannot lead to unstable fluid-body interactions in which the body spontaneously accelerates indefinitely.

IX. CONCLUSION

The well-known decomposition of aerodynamic force into added-mass and circulatory components has its origins in potential flow theory. In the classical decomposition, shed vorticity is represented by vortex singularities, whose associated potential can be linearly superimposed onto the single-valued potential which gives rise to the added-mass force. The present work shows that this decomposition is also valid for viscous, separated flows containing continuous distributions of vorticity, as demonstrated by means of a Helmholtz decomposition of the velocity field. The resulting equations are valid for an impermeable body of arbitrary geometry, in two or three dimensions, undergoing arbitrary motion through an unbounded, incompressible fluid domain. The force acting on the body is related to the time derivative of total impulse $\mathbf{P}$ defined as

$$\mathbf{P} = \mathbf{P}_v + \mathbf{P}_i + \mathbf{P}_\phi + \mathbf{P}_b.$$

The four terms on the right-hand side are the shed-vorticity impulse, the image-vorticity impulse, the potential impulse, and the body-volume impulse, respectively. Upon time differentiation, the first two terms give rise to the circulatory force and the latter two combine to give the classical added-mass force. The generality of the derivation demonstrates that the added-mass force is a valid component of total force regardless of the presence of a vortical wake. The presented force formulation was shown to be equivalent to existing theoretical work, under the specific conditions and assumptions of previous studies [2,5,7,21,23]. The force formulation was also validated using a numerical data set generated by Wang and Eldredge [21], wherein the flow around a pitching plate in a steady freestream was simulated. The calculated force shows fairly good agreement with the force reported by Wang and Eldredge [21], although minor discrepancies indicate that further work must be done to quantify errors due to discretization.

When the no-slip condition holds, it was shown that the total impulse can be equivalently expressed as

$$\mathbf{P} = \mathbf{P}_v + \mathbf{P}_b,$$

which indicates that the no-slip condition causes the potential impulse and image-vorticity impulse terms to cancel for all time, i.e., $\mathbf{P}_i + \mathbf{P}_\phi \equiv 0$. Such cancellation was indeed shown to hold in the Wang-Eldredge data set [21]. This relationship could prove valuable to future predictive aerodynamic models; the potential impulse can be calculated for all time *a priori* based on body geometry and motion, which in turn places an integral restriction on the evolution of the vorticity field.

Two key insights regarding the classical added-mass force were emphasized. First, for bodies of nonzero volume, the added-mass force differs depending on whether body itself accelerates or whether the freestream flow accelerates relative to the body. This is a known phenomenon in the marine literature, but may be overlooked in other fields. Second, the most general expression for the added-mass force acting on an accelerating flat plate includes a tangential component.

Misinterpretations of added mass persist in the literature, wherein the added-mass force is attributed to the acceleration of fluid that must move with the body. By inspection of the derived impulse terms, the authors adhere to the more physically accurate interpretation that the added-mass force accounts for the dynamic effect of the near-body vorticity distribution, without defining a specific contour or associated region of fluid. This interpretation arises due to the cancellation of the shed-vorticity and image-vorticity impulse terms near the body surface. Such cancellation reduces the importance of acquiring accurate near-body vorticity data, which could be advantageous in application to experimental data sets. Investigation of the experimental utility of the presented force formulation is left for future work.

ACKNOWLEDGMENT

The authors would like to thank the Natural Sciences and Engineering Research Council of Canada for their financial backing.

APPENDIX A: PROOF THAT $\int_{V_b} \nabla \times \boldsymbol{\psi}' dV = 0$ IN TWO AND THREE DIMENSIONS DUE TO THE IMPERMEABLE BOUNDARY CONDITION

In the derivation in Sec. II, it was claimed that

$$\int_{V_b} \nabla \times \boldsymbol{\psi}' dV = 0 \tag{A1}$$

due to the impermeable boundary condition, which will now be proven first in three dimensions and then in two. The boundary condition demands that

$$\hat{n} \cdot (\nabla \times \boldsymbol{\psi}') = 0 \tag{A2}$$

on the body surface S_b. It can thus be stated that

$$\int_S \hat{n} \cdot (\nabla \times \boldsymbol{\psi}') dS = 0 \tag{A3}$$

for any surface $S \subset S_b$. Consider a plane M which intersects the volume V_b and let D be the cross section of the body on M, bounded by one or more closed curves $\{L_i\}$, which jointly make up the boundary ∂D (see Fig. 6). The surface S_b is thus divided into two sets of one or more surfaces on either side of M; let us denote one of these sets by $\{S_i\}$. Each S_i serves as a capping surface for one or more L_i and by Stokes's theorem,

$$\begin{aligned} 0 &= \sum_i \int_{S_i} \hat{n} \cdot (\nabla \times \boldsymbol{\psi}') dS \\ &= \sum_i \int_{L_i} \hat{n} \cdot \boldsymbol{\psi}' ds \\ &= \int_{\partial D} \hat{n} \cdot \boldsymbol{\psi}' ds \\ &= \int_D \hat{n_d} \cdot (\nabla \times \boldsymbol{\psi}') dD, \end{aligned} \tag{A4}$$

where $\hat{n}_d$ is a unit normal on D and the integral over each S_i vanishes due to Eq. (A3).

The volume integral in Eq. (A1) can be evaluated by dividing the domain into infinitesimally thin slices, each slice being a cross section D, parallel to each other's cross section, with thickness dl. The elemental volume in Eq. (A1) is thus expressed as $dV = dDdl$ and the volume integral can be

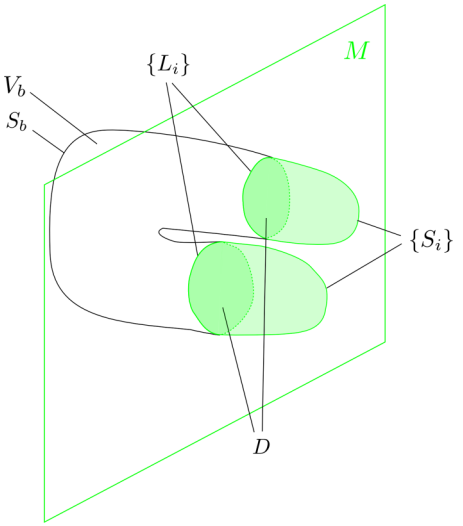

FIG. 6. The plane M intersects the arbitrary body occupying volume V_b, generating the cross section D bounded by the closed curves $\{L_i\}$. The surfaces $\{S_i\} \subset S_b$, which exist on one side of M, act as capping surfaces on the closed curves $\{L_i\}$, permitting the application of Stokes's theorem.

rewritten as

$$\int_{V_b} \nabla \times \boldsymbol{\psi}' dV = \int \left[\int_D \nabla \times \boldsymbol{\psi}' dD \right] dl. \tag{A5}$$

The outer integral is to be evaluated over the dimension normal to each cross section D. The unit normal $\hat{n}_d$ is constant over each cross section such that

$$\hat{n}_d \cdot \left(\int_{V_b} \nabla \times \boldsymbol{\psi}' dV \right) = \int \left[\int_D \hat{n}_d \cdot (\nabla \times \boldsymbol{\psi}') dD \right] dl = 0, \tag{A6}$$

which vanishes by Eq. (A4). Since the orientation of $\hat{n}_d$ can be set arbitrarily, this equation can only hold if $\int_{V_b} \nabla \times \boldsymbol{\psi}' dV = 0$.

In two dimensions, $\boldsymbol{\psi}' = \psi' \hat{k}$ on V_b and S_b, where $\hat{k}$ is normal to the two-dimensional plane. The impermeable boundary condition can thus be expressed as

$$\frac{\partial \psi'}{\partial s} = 0, \tag{A7}$$

where s denotes the tangential direction on S_b. We relate the integral over the body to a surface integral according to the identity [37]

$$\int_{V_b} \nabla \times \boldsymbol{\psi}' dV = \int_{S_b} \hat{n} \times \boldsymbol{\psi}' dS. \tag{A8}$$

Due to Eq. (A7), ψ' is constant on S_b such that

$$\int_{S_b} \hat{n} \times \boldsymbol{\psi}' dS = \left(\int_{S_b} \hat{n} dS \right) \times \boldsymbol{\psi}' = 0 \tag{A9}$$

and therefore $\int_{V_b} \nabla \times \boldsymbol{\psi}' dV = 0$ by Eq. (A8).

APPENDIX B: INVARIANCE OF TOTAL VORTICAL IMPULSE TO INFINITY-PRESERVING CONFORMAL TRANSFORMATIONS

Consider a two-dimensional incompressible fluid domain V bounded internally by the surface of a solid body S_b and externally by the contour S_∞ at infinity. The velocity within V can be decomposed according to a Helmholtz decomposition, as given in Eq. (12). We define the rotational component of the flow field to be $\mathbf{u}_v = \nabla \times \boldsymbol{\psi}$ and extend the velocity field into the body volume V_b. We can invoke the impulse-momentum identity in Eq. (11) to express the momentum associated with the $\mathbf{u}_v$ field in the combined domain $V + V_b$ as

$$\int_{V+V_b} \mathbf{u}_v dV = \int_{V+V_b} \mathbf{x} \times \boldsymbol{\omega}\, dV - \oint_{S_\infty} \mathbf{x} \times (\hat{n} \times \mathbf{u}_v) dS \tag{B1}$$

$$= \int_{V+V_b} \nabla \times \boldsymbol{\psi}\, dV. \tag{B2}$$

The integral in Eq. (B2) can be transformed to a contour integral on S_∞ by the identity in Eq. (A8) such that the total vortical impulse can be expressed as

$$\int_{V+V_b} \mathbf{x} \times \boldsymbol{\omega}\, dV = \oint_{S_\infty} [\hat{n} \times \boldsymbol{\psi} + \mathbf{x} \times (\hat{n} \times \mathbf{u}_v)] dS. \tag{B3}$$

If we conformally map the velocity field $\mathbf{u}_v$ to another domain in which the impulse-momentum identity still holds and if we choose the map such that it has no effect at infinity, the right-hand side of Eq. (B3) remains unchanged. Therefore, the total vortical impulse, as represented on the left-hand side of Eq. (B3), will be invariant to any such conformal transformation.

[1] T. Theodorsen, General theory of aerodynamic instability and the mechanism of flutter, National Advisory Committee for Aeronautics Report No. 496, 1935 (unpublished).

[2] T. von Kármán and W. R. Sears, Airfoil theory for non-uniform motion, J. Aeronaut. Sci. **5**, 379 (1938).

[3] G. G. Stokes, On the effect of the internal friction of fluids on the motion of pendulums, Trans. Cambridge Philos. Soc. **9**, 8 (1851).

[4] C. E. Brennen, A review of added mass and fluid inertial forces, Naval Civil Engineering Laboratory Report No. CR 82.010, 1982 (unpublished).

[5] J. C. Wu, Theory for aerodynamic force and moment in viscous flows, AIAA J. **19**, 432 (1981).

[6] P. G. Saffman, *Vortex Dynamics* (Cambridge University Press, Cambridge, 1992).

[7] J. Lighthill, Fundamentals concerning wave loading on offshore structures, J. Fluid Mech. **173**, 667 (1986).

[8] H. Lamb, *Hydrodynamics*, 6th ed. (Dover, New York, 1932).

[9] J. Katz and A. Plotkin, *Low-Speed Aerodynamics*, 2nd ed. (Cambridge University Press, Cambridge, 2001).

[10] S. L. Brunton and C. W. Rowley, Empirical state-space representations for Theodorsen's lift model, J. Fluids Struct. **38**, 174 (2013).

[11] J. J. Thomson, *A Treatise on the Motion of Vortex Rings* (Macmillan, New York, 1883).

[12] J.-Z. Wu, H.-Y. Ma, and M.-D. Zhou, *Vortical Flows* (Springer, Berlin, 2015).

[13] J. M. Burgers, On the resistance of fluids and vortex motion, Proc. K. Ned. Akad. Wet. **23**, 774 (1921).

[14] J. Lighthill, *An Informal Introduction to Theoretical Fluid Mechanics* (Oxford University Press, New York, 1986).

[15] J.-C. Lin and D. Rockwell, Force identification by vorticity fields: Techniques based on flow imaging, J. Fluids Struct. **10**, 663 (1996).

[16] J.-Z. Wu, X.-Y. Lu, and L.-X. Zhuang, Integral force acting on a body due to local flow structures, J. Fluid Mech. **576**, 265 (2007).

[17] A. Mohebbian and D. E. Rival, Assessment of the derivative-moment transformation method for unsteady-load estimation, Exp. Fluids **53**, 319 (2012).
[18] A. C. DeVoria, Z. R. Carr, and M. J. Ringuette, On calculating forces from the flow field with application to experimental volume data, J. Fluid Mech. **749**, 297 (2014).
[19] D. E. Rival and B. van Oudheusden, Load-estimation techniques for unsteady incompressible flows, Exp. Fluids **58**, 20 (2017).
[20] X. Xia and K. Mohseni, Lift evaluation of a two-dimensional pitching flat plate, Phys. Fluids **25**, 091901 (2013).
[21] C. Wang and J. D. Eldredge, Low-order phenomenological modeling of leading-edge vortex formation, Theor. Comput. Fluid Dyn. **27**, 577 (2013).
[22] K. Ramesh, A. Gopalarathnam, J. R. Edwards, M. V. Ol, and K. Granlund, An unsteady airfoil theory applied to pitching motions and validated against experiment and computation, Theor. Comput. Fluid Dyn. **27**, 843 (2013).
[23] D. T. Polet, D. E. Rival, and G. D. Weymouth, Unsteady dynamics of rapid perching manoeuvres, J. Fluid Mech. **767**, 323 (2015).
[24] F. Noca, On the evaluation of time-dependent fluid-dynamic forces on bluff bodies, Ph.D. thesis, California Institute of Technology, 1997.
[25] F. Noca, D. Shiels, and D. Jeon, A comparison of methods for evaluating time-dependent fluid dynamic forces on bodies, using only velocity fields and their derivatives, J. Fluids Struct. **13**, 551 (1999).
[26] F. Noca, Apparent mass in viscous, vortical flows, *Proceedings of the 54th Annual Meeting of the APS Division of Fluid Dynamics* (APS, San Diego, CA, 2001).
[27] D. Shiels, A. Leonard, and A. Roshko, Flow-induced vibration of a circular cylinder at limiting structural parameters, J. Fluids Struct. **15**, 3 (2001).
[28] S. J. Colley, *Vector Calculus*, 4th ed. (Pearson, Hoboken, 2012).
[29] J.-Z. Wu, H.-Y. Ma, and M.-D. Zhou, *Vorticity and Vortex Dynamics* (Springer, Berlin, 2006).
[30] E. Konstantinidis, Added mass of a circular cylinder oscillating in a free stream, Proc. R. Soc. A **469**, 20130135 (2013).
[31] R. R. Clements, An inviscid model of two-dimensional vortex shedding, J. Fluid Mech. **57**, 321 (1973).
[32] A. M. Kuethe and C.-Y. Chow, *Foundations of Aerodynamicsmil*, 5th ed. (Wiley, New York, 1998).
[33] L. M. Milne-Thompson, *Theoretical Hydrodynamics*, 4th ed. (MacMillan, New York, 1960).
[34] J. D. Eldredge, Numerical simulation of the fluid dynamics of 2D rigid body motion with the vortex particle method, J. Comput. Phys. **221**, 626 (2007).
[35] J. N. Fernando and D. E. Rival, On the dynamics of perching manoeuvres with low-aspect-ratio planforms, Bioinspir. Biomim. **12**, 046007 (2017).
[36] J. Kriegseis and D. E. Rival, Vortex force decomposition in the tip region of impulsively-started flat plates, J. Fluid Mech. **756**, 758 (2014).
[37] H. M. Schey, *Div, Grad, Curl and All That*, 2nd ed. (W. W. Norton and Company, Inc., New York, 1992).